

## Article

# Effective Removal of Acetaldehyde Using Piperazine/Nitric Acid Co-Impregnated Bead-Type Activated Carbon

Yu-Jin Kang <sup>1</sup>, Yu-Jin Kim <sup>1</sup>, Seong-Jin Yoon <sup>1</sup>, Dong-Jin Seo <sup>1</sup>, Hye-Ryeong Cho <sup>1</sup>, Kyeongseok Oh <sup>2</sup> ,  
Seong-Ho Yoon <sup>3,\*</sup>  and Joo-Il Park <sup>1,\*</sup>

- <sup>1</sup> Department of Chemical & Biological Engineering, Hanbat National University, Daejeon 34158, Republic of Korea; yujin0581@naver.com (Y.-J.K.); yzyy0840@naver.com (Y.-J.K.); tjdwls7856@gmail.com (S.-J.Y.); tjehdwls0963@naver.com (D.-J.S.); ryeong2829@gmail.com (H.-R.C.)
- <sup>2</sup> Department of Chemical & Biological Engineering, Inha Technical College, Incheon 22212, Republic of Korea; kyeongseok.oh@inhac.ac.kr
- <sup>3</sup> Interdisciplinary Graduate School of Engineering Science, Kyushu University, Fukuoka 816-8580, Japan
- \* Correspondence: yoon@cm.kyushu-u.ac.jp (S.-H.Y.); jipark94@hanbat.ac.kr (J.-I.P.);  
Tel.: +81-92-583-7959 (S.-H.Y.); +82-42-821-1530 (J.-I.P.)

**Abstract:** Acetaldehyde (CH<sub>3</sub>CHO) in the atmosphere is associated with adverse health effects. Among the various options for use in removing CH<sub>3</sub>CHO, adsorption is often employed because of its convenient application and economical processes, particularly when using activated carbon. In previous studies, the surface of activated carbon has been modified with amines to remove CH<sub>3</sub>CHO from the atmosphere via adsorption. However, these materials are toxic and can have harmful effects on humans when the modified activated carbon is used in air-purifier filters. Therefore, in this study, a customized bead-type activated carbon (BAC) with surface modification options via amination was evaluated for removing CH<sub>3</sub>CHO. Various amounts of non-toxic piperazine or piperazine/nitric acid were used in amination. Chemical and physical analyses of the surface-modified BAC samples were performed using Brunauer–Emmett–Teller measurements, elemental analyses, and Fourier transform infrared and X-ray photoelectron spectroscopy. The chemical structures on the surfaces of the modified BACs were analyzed in detail using X-ray absorption spectroscopy. The amine and carboxylic acid groups on the surfaces of the modified BACs are critical in CH<sub>3</sub>CHO adsorption. Notably, piperazine amination decreased the pore size and volume of the modified BAC, but piperazine/nitric acid impregnation maintained the pore size and volume of the modified BAC. In terms of CH<sub>3</sub>CHO adsorption, piperazine/nitric acid impregnation resulted in a superior performance, with greater chemical adsorption. The linkages between the amine and carboxylic acid groups may function differently in piperazine amination and piperazine/nitric acid treatment.

**Keywords:** bead-type activated carbon; piperazine; nitric acid; surface modification; acetaldehyde removal



**Citation:** Kang, Y.-J.; Kim, Y.-J.; Yoon, S.-J.; Seo, D.-J.; Cho, H.-R.; Oh, K.; Yoon, S.-H.; Park, J.-I. Effective Removal of Acetaldehyde Using Piperazine/Nitric Acid Co-Impregnated Bead-Type Activated Carbon. *Membranes* **2023**, *13*, 595. <https://doi.org/10.3390/membranes13060595>

Academic Editor: Daqi Cao

Received: 10 May 2023

Revised: 8 June 2023

Accepted: 10 June 2023

Published: 12 June 2023



**Copyright:** © 2023 by the authors. Licensee MDPI, Basel, Switzerland. This article is an open access article distributed under the terms and conditions of the Creative Commons Attribution (CC BY) license (<https://creativecommons.org/licenses/by/4.0/>).

## 1. Introduction

Acetaldehyde (CH<sub>3</sub>CHO) is a volatile organic compound (VOC) in the atmosphere that is associated with adverse health effects. It is a factor in sick building syndrome, as it is found in wallpaper, furniture, cigarettes, and building materials [1–8]. Moreover, CH<sub>3</sub>CHO is odorous at a low concentration (0.09 mg/m<sup>3</sup>) and causes chest tightness, eye irritation, and respiratory tract irritation [9,10]. Therefore, indoor CH<sub>3</sub>CHO content should be regulated at <0.03 ppm, and an effective removal method for CH<sub>3</sub>CHO is required [11].

Several methods, such as absorption [12], condensation [13], biofiltration [14], and thermal oxidation [15], are commonly applied in removing VOCs such as CH<sub>3</sub>CHO, from gas streams. These methods are effective at relatively high VOC concentrations

(>5000 ppmv) [16], but adsorption yields the optimal results in terms of energy cost, efficiency, and versatility with respect to the adsorbate [17]. Adsorption is one of the most efficient methods of removing VOCs, and various adsorbents are used, including carbon materials [18], silica [19], zeolites [20], and polymers [21]. Owing to their low costs and high stabilities, carbon materials are the most commonly used adsorbents in VOC removal [22]. Activated carbon, in particular, provides key advantages in adsorption because of its high porosity, large surface area, and rapid adsorption [23,24]. It is well-known that the intrinsic surface of activated carbon is hydrophobic. However, in many cases, the operation of activated carbon requires a hydrophilic environment such as water purification and wastewater treatment. Even VOC removal occurs in humid environments. Among the options of surface modification, acidic treatments are popular. Strong acids such as nitric acid are often used in surface modification. With the help of acidic treatment, the generation of carboxylic acid is noticeable along with hydroxyl groups. With the increasing need to remove specific chemicals such as aldehydes, the refined surface modification was necessitated with or without acidic treatment. Amination showed promising results in formaldehyde removal [18]. Previous studies have reported on the surface modification of activated carbon with amines that can be used to remove  $\text{CH}_3\text{CHO}$  from the atmosphere. The amine-containing materials used in previous studies include aminobenzenesulfonic acids, ethylenediamine, diethylenetriamine, and amino acids [25–27]. However, these materials are toxic and can have harmful effects on humans when the modified activated carbon is used in air-purifier filters. Therefore, developing non-toxic amine-modified activated carbon is essential, but no related research regarding the adsorption of  $\text{CH}_3\text{CHO}$  with non-toxic amines has been reported. In addition, the related references on acetaldehyde removal over activated carbon materials are summarized in Table 1.

In this study, we used a spherical bead-type activated carbon (BAC), which provides a pleasant working environment with no dust and high strength and fluidity. This type of BAC can be easily operated for adsorption and desorption, thereby making it feasible for recycling and helping for a circular economy. Specifically, compared to commercial granular activated carbon, BAC has a narrow-sized distribution. If BAC is applied to a BAC-incorporated membrane filter, a new design of the cartridge-type filter can be proposed. For a better understanding, the overall concept of BAC application is presented in Figure 1. Due to these properties, BAC is particularly useful as an air-purifier filter, and further research is necessary to explore its applicability [28]. The main aim of this study is to characterize the detailed adsorption behavior of  $\text{CH}_3\text{CHO}$  over BAC modified with piperazine, which is a non-toxic amine. Moreover, the reaction mechanism of  $\text{CH}_3\text{CHO}$  removal using the non-toxic amine-BAC is investigated in detail.

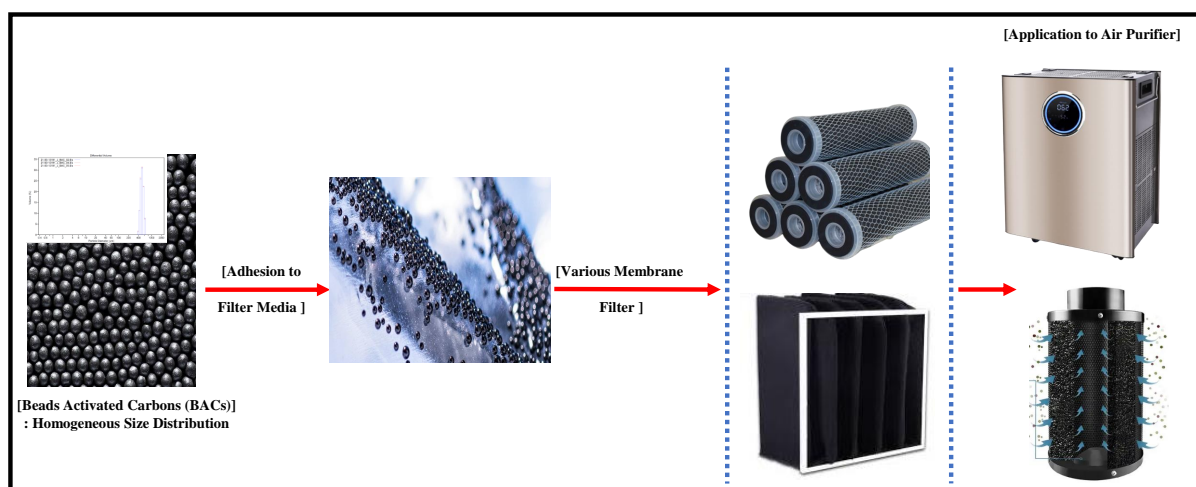


**Figure 1.** Conceptual illustration of BACs applied to air purification through systemizing membrane filtration.

**Table 1.** The related research on acetaldehyde removal using activated carbon.

References	Activated Carbon Type	Impregnated Material	Mechanism
[29]	AC (Calgon, Norit, and Westvaco)	nitric acid	(1) When very small pores as close as the size of the acetaldehyde molecule and oxygen-containing groups are present (to a certain extent) within AC, the heat of adsorption reaches its maximum value. (2) A low density of surface groups can enhance the heat of adsorption, whereas extensive oxidation leads to a decrease in the strength of adsorption forces. This happens due to the blockage of the pore entrances containing functional groups and the decrease in the accessibility of hydrophobic surface where the dispersive interactions of hydrocarbon moiety can be enhanced.
[30]	AC (Calgon and Westvaco)	urea (450/950 °C)	(1) The adsorption forces are strong in small pores, and their volume governs the adsorbed amount. (2) The absorbed amount can be enhanced when functional groups bearing nitrogen are present. (3) These groups can provide additional adsorption centers when the small pores are filled with acetaldehyde molecules.
[26]	AC (coconut-shell and coal-base)	amine	$2 \text{CH}_3\text{CHO} \longrightarrow \text{CH}_3\text{CH}=\text{CH}-\text{CHO} + \text{H}_2\text{O}$
[31]	AC (corn grain)	KOH	(1) The effects of acetaldehyde adsorption on ACs were investigated in terms of textural properties, energetic heterogeneity, and surface chemistries. (2) The adsorption properties of water vapor were explained by the effect of the oxygen-containing groups on the surface of ACs over acetaldehyde adsorption. (3) The influences of pore size distribution (below 8 Å) and energetic heterogeneity of ACs on acetaldehyde adsorption were highly predominant compared to that of specific surface area and surface chemistry.
[32]	AC (coconut base)	-	The study established a semi-quantitative relationship between pore size distribution and energy in relation to adsorption kinetics; the wider and more heterogeneous porosities resulted in higher rate constants for the resin-based carbon when compared to the ultramicroporous nutshell material.
[33]	ACF	metal oxide	ACF-K-20/5%MgO revealed three types of surface adsorption sites: one was assigned to physisorption on the surface O-containing carbon groups and two other sites are placed on a MgO surface and provide acetaldehyde chemisorption in two different modes.
[34]	ACF (cellulose base)	aniline-ethanol	(1) $\text{CH}_3\text{CHO}_{(\text{g})} \rightarrow \text{CH}_3\text{CHO}_{(\text{AD})}$ [Adsorption] (2) $\text{CH}_3\text{CHO}_{(\text{AD})} + \frac{1}{2}\text{O}_2 \rightarrow \text{CH}_3\text{COOH}$ [Oxidation] (3) $2\text{CH}_3\text{COOH} \rightarrow (\text{CH}_3\text{CO})_2\text{O} + \text{H}_2\text{O}$ [Dehydration] (4) $(\text{CH}_3\text{CO})_2\text{O} + \text{C}_6\text{H}_5\text{NH}_2 \rightarrow \text{C}_6\text{H}_5\text{NCH}_3\text{CO} - \text{CH}_3\text{COOH}$
[35]	ACF (HDPE fiber)	Ag	(1) Ag particles were precipitated on the surface of ACF through interactive affinity, and the carbonyl group of AA is increased to show that AA is adsorbed on the AC surface. (2) The AA adsorption of ACF and Ag/ACF composites performed in this study was suitable for the dose–response model, and the experimental data showing the asymmetric shape of the AA adsorption breakthrough curve for ACF and Ag/ACF composites were satisfactorily fitted.
[36]	AC and ACF	amine	(1) The high BET surface area provides more sites for acetaldehyde adsorption. (2) ACF has a systematic open macrostructure, which drives a low-pressure drop and allows fast adsorption without diffusion hindrance.

## 2. Experimental Section

### 2.1. Materials and Sample Preparation

BAC (particle diameter of <0.1 mm) was obtained from ZEOBuilder (Seoul, Republic of Korea) and heated at 900 °C for 3 h under N<sub>2</sub> flowing at 175 mL/min.

Piperazine, nitric acid, and ethyl alcohol were purchased from Samchun Pure Chemical (Pyeongtaek, Republic of Korea). Piperazine was prepared with ethyl alcohol, and nitric acid was prepared with distilled water. Aqueous stock solutions containing 1–10% (*w/v*) piperazine with or without 1% (*w/v*) nitric acid were prepared. The sample names differ according to the contents of the mixtures used (Table 2). The heated BAC was impregnated with the solution of piperazine with/without nitric acid, and the sample was then placed in a shaking water bath at 25 °C and shaken at 130 rpm for 24 h. After impregnation, the BAC was filtered and dried at 70 °C for 24 h. For comparison, piperazine was impregnated on coconut shell and coal-based activated carbons using the same procedure (Supplementary Information Figure S8).

**Table 2.** Description of each sample.

Sample	Piperazine % [ <i>w/v</i> %]	Nitric Acid % [ <i>w/v</i> %]	Heat Treatment Temp. [°C]
P1	1	-	-
P7	7	-	-
P7N1	7	1	-
P1N1-900	1	1	900
P3N1-900	3	1	900
P5N1-900	5	1	900
P7N1-900	7	1	900
P10N1-900	10	1	900

### 2.2. Methods

#### 2.2.1. Preliminary Characterization of BACs

In order to investigate the characteristics of acetaldehyde removal for the BACs impregnated with piperazine/nitric acid, BARE-BAC was first examined by XRD, SEM, TEM, EDX, particle size distribution, as well as physical/chemical stability. All data is presented in the Supplementary Information (Figures S1–S7). In brief, BARE-BAC showed the amorphous phase (refer to XRD data in the Supplementary Information) without any crystallinity, therefore Raman characteristics were not necessary to verify its further crystallinity. BAC from a resin precursor contains a slight impurity of Si, characterized by SEM-EDX. Basically, approx. 1 wt% of impurity in activated carbon cannot affect its adsorption capacity. SEM morphology implies that the BACs were successfully synthesized from the resin precursor. The narrow window of particle size distribution in BARE-BAC ranged from 440 to 600 μm with a mean value of 512 μm, indicating homogeneous particle size compared with commercial granular activated carbon. It can be easily applied to the various type of membrane filter system. Moreover, the physical stability has been tested by attrition and abrasion (ASTM D4058-96 & SPENCE Method). Two tests were performed which showed the value of 99.77 with a deviation of 0.11. The acetaldehyde cycle test was carried out to confirm the chemical stability. The regeneration efficiency showed about 90% during 3 cycles of the adsorption–desorption process under the given operational conditions (200 ppm, GHSV: 37,500 h<sup>-1</sup>, 25 °C).

#### 2.2.2. N<sub>2</sub> Sorption

N<sub>2</sub> adsorption–desorption isotherms were obtained at 77 K using a surface area and pore size analyzer (BELSORP MAX G, Microtrac MRB, Osaka, Japan). Before the adsorption studies, the BAC was outgassed at 120 °C under vacuum for 8 h. The surface area was determined using the Brunauer–Emmett–Teller (BET) equation, the total pore volume was

calculated at a relative pressure ( $P/P_0$ ) of 0.99, and the micropore volume was calculated using the Horvath–Kawazoe (HK) and t-plot methods.

### 2.2.3. CHNS Elemental Analysis

A CHNS elemental analyzer (Flash 2000, Thermo Fisher Scientific, Waltham, MA, USA) with a thermal conductivity detector was used to examine the compositions of the BAC samples to determine the relative contents of C, H, N, and S as percentages.

### 2.2.4. Fourier Transform Infrared (FTIR) Spectroscopy

FTIR spectroscopy was used to qualitatively evaluate the chemical structures of the BAC samples. The FTIR spectra were measured using an FTIR spectrometer (US/iS50, Thermo Fisher Scientific) in the frequency range of 400–4000  $\text{cm}^{-1}$ .

### 2.2.5. X-ray Photoelectron Spectroscopy (XPS)

XPS was performed using an XP spectrometer (K-Alpha<sup>+</sup>, Thermo Fisher Scientific) with a monochromatic Al  $K\alpha$  (1486.6 eV) radiation source operated at 15 kW and 50 W. Prior to the analysis, the samples were outgassed at room temperature until the system pressure reached  $5.2 \times 10^{-9}$  torr. High-resolution spectra were collected at a constant pass energy of 29.35 eV over an area with a diameter of 4000  $\mu\text{m}$ . The amount of each element (C, O, N, and S) was calculated using individual spectrum, and the energy scale was calibrated using the C 1s photoelectron line at 285.0 eV.

### 2.2.6. CH<sub>3</sub>CHO Adsorption

Figure 2 schematically illustrates the continuous flow system employed in evaluating CH<sub>3</sub>CHO removal using the BAC samples. Tests were conducted at 10 °C using a thermo-hygrostat (climatic chamber, Weiss Technik, Rieskirchen-Lindenstruth, Germany), and the BAC sample (2 mL) was placed in a stainless steel column. The CH<sub>3</sub>CHO gas was 1000 ppm CH<sub>3</sub>CHO in N<sub>2</sub>, which was then mixed with air to yield a CH<sub>3</sub>CHO concentration of 200 ppm. Gas analysis was performed using a sampling pump (GV-100S, Gastec, Ayase, Japan) and tube (92/92M/92L, Gastec). The breakthrough adsorption capacity of CH<sub>3</sub>CHO ( $W_{\text{ad}}$  [mg/g]) was calculated by integrating the area under the breakthrough curve using the flow rate, CH<sub>3</sub>CHO concentration, time, and adsorbent mass. All adsorption tests were stopped at  $C_{\text{out}}/C_{\text{in}} = 1$  ( $C_{\text{out}}$  [ppm]: outlet concentration of CH<sub>3</sub>CHO;  $C_{\text{in}}$  [ppm]: inlet concentration of CH<sub>3</sub>CHO).

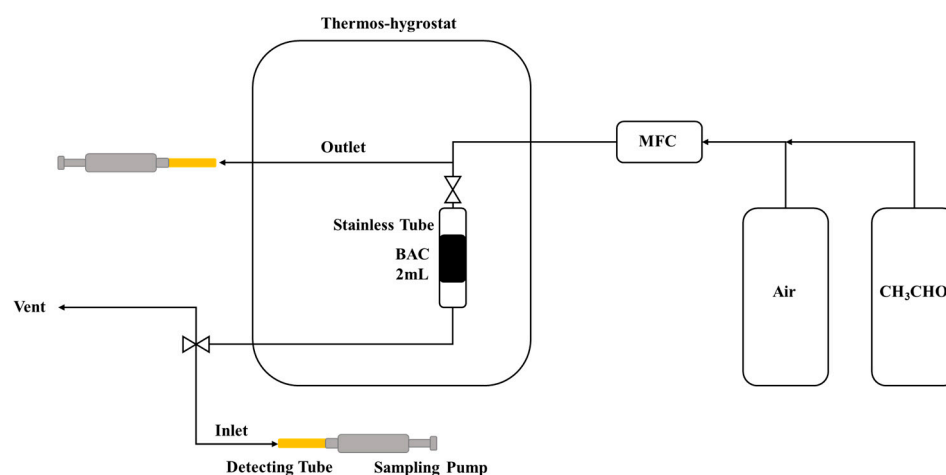


**Figure 2.** Schematic illustration of our CH<sub>3</sub>CHO removal apparatus for lab-scale tests.

### 2.2.7. Thermal Regeneration

The modified BACs were thermally regenerated in a muffle furnace (Daihan Scientific, Wonju, Republic of Korea). After the CH<sub>3</sub>CHO adsorption studies, the spent BAC samples

(approximately 2 mL) were heated from room temperature to 453 K (heating rate: 5 K/min) and maintained at this temperature for 2 h in air.

### 3. Results

#### 3.1. Characterizations of BAC

##### 3.1.1. Textural Structure

The textural properties of the BAC samples, which were determined using the N<sub>2</sub> adsorption–desorption isotherms, are summarized in Table 3. The BET surface areas ( $S_{\text{BET}}$ ) decrease in the following order: BARE-BAC > piperazine/nitric acid-co-impregnated BACs > piperazine-modified BACs. Piperazine treatment decreases the  $S_{\text{BET}}$  of BARE-BAC, but the co-impregnation with piperazine and nitric acid minimizes the decrease, likely because the nitric acid molecules adsorbed on the pore surfaces continue to penetrate the pore walls during impregnation. However, as the piperazine content increases, the pores of the BAC are blocked, and  $S_{\text{BET}}$  decreases. BARE-BAC displays the highest  $S_{\text{BET}}$  (1442.1 m<sup>2</sup>/g) and the highest micropore and total pore volumes (0.6189 and 0.6284 cm<sup>3</sup>/g, respectively), which are almost 6–77% higher than those of the modified BACs. Therefore, chemical factors have a greater effect on CH<sub>3</sub>CHO adsorption than physical factors.

**Table 3.** Textural properties of BAC samples.

Sample	$S_{\text{BET}}$ [m <sup>2</sup> /g]	$S_{\text{Micro}}$ [m <sup>2</sup> /g]	$V_{\text{Total}}$ [cm <sup>3</sup> /g]	$V_{\text{Micro}}$ [cm <sup>3</sup> /g]	Average Pore Diameter [nm]
BARE-BAC	1442.1	1437.3	0.6284	0.6189	1.7429
P1	921.5	916.9	0.4123	0.4033	1.7898
P7	794.5	791.0	0.3533	0.3462	1.7788
P7N1	1141.3	1137.1	0.5001	0.4916	1.7528
P1N1-900	1347.2	1341.2	0.5905	0.5788	1.7533
P3N1-900	1275.3	1270.2	0.5612	0.5508	1.7602
P5N1-900	1191.6	1185.8	0.5259	0.5142	1.7652
P7N1-900	1115.3	1110.0	0.4818	0.4711	1.7281
P10N1-900	983.8	979.3	0.4390	0.4298	1.7850

The piperazine/nitric acid-co-impregnated BACs exhibit larger micropore volumes than the piperazine-modified BACs. Overall, co-impregnation with piperazine and nitric acid should result in different modifications of the BAC surface compared to those caused by piperazine modification of the BAC.

##### 3.1.2. CHNS Elemental Analysis

The contents of C, H, N, and S in the samples were measured using a CHNS elemental analyzer, and the results are shown in Table 4. The N and H contents increase after treatment with piperazine and nitric acid, respectively, and the introduced amine (–NH) groups are critical in CH<sub>3</sub>CHO removal via chemisorption [26,27,34].

**Table 4.** Contents of C, H, N, and S in BAC samples.

Sample	C [%]	H [%]	N [%]	S [%]
BARE-BAC	93.84	0.45	* ND	1.31
P1	80.18	2.16	0.63	1.01
P7	87.00	1.64	3.52	1.13
P7N1	85.90	1.74	1.89	1.21
P1N1-900	83.02	2.30	0.39	0.97
P3N1-900	93.39	0.79	1.23	1.25
P5N1-900	81.99	2.67	1.52	0.94
P7N1-900	83.21	2.21	2.13	0.98
P10N1-900	80.89	2.77	2.67	0.89

\* ND: No data.

### 3.1.3. Chemical Characterization

Figure 3 shows the FTIR spectra of BARE-BAC and P7N1-900, which adsorbs the highest amount of  $\text{CH}_3\text{CHO}$ . The characteristic peaks attributed to the functional groups are almost identical in the two spectra. The O–H and N–H bonds result in noticeable peaks, and Table 5 summarizes the intensity data of the functional groups. The spectrum of P7N1-900 displays peaks with stronger intensities the O–H and amine functional groups representing treatment with piperazine and nitric acid. Penchah et al. [37] reported that nitric acid increases the carboxylic acid (COOH) content on the surface of activated carbon, and piperazine is linked to COOH. Therefore, the number of OH groups of P7N1-900 is increased approximately 2-fold on account of using nitric acid, and the number of amine groups is increased approximately 4.2-fold on account of using piperazine. In addition, no change in the structure of BAC is observed, as there is almost no change in the  $-\text{CH}_2$  groups.

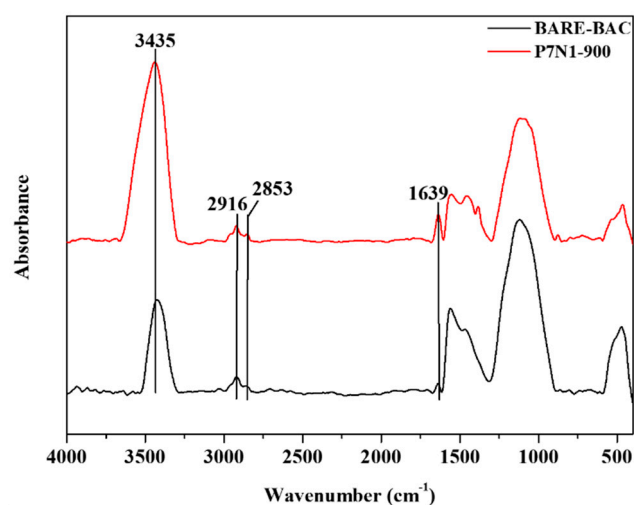


Figure 3. FTIR spectrum of BARE-BAC and P7N1-900.

Table 5. Intensity of BARE-BAC and P7N1-900's functional groups.

Band Position [ $\text{cm}^{-1}$ ]	Component	Intensity	
		BARE-BAC	P7N1-900
3435	O-H	3.40	6.95
2916	Saturated aliphatic $\text{CH}_2$	0.42	0.46
2853	Saturated aliphatic $\text{CH}_2$	0.16	0.21
1639	Amine, primary/secondary NH	0.29	1.23

Sources: Adapted from [38].

Ryu et al. [34] reported that the amine functional groups on activated carbon lead to a higher  $\text{CH}_3\text{CHO}$  adsorption efficiency, and thus, the amine groups should increase  $\text{CH}_3\text{CHO}$  adsorption.

### 3.1.4. XPS

XPS was used to investigate the chemical states of the elements in the BAC samples. The deconvoluted spectra are shown in Figure 4, and the relative abundances of C, O, N, and S are presented in Table 6.

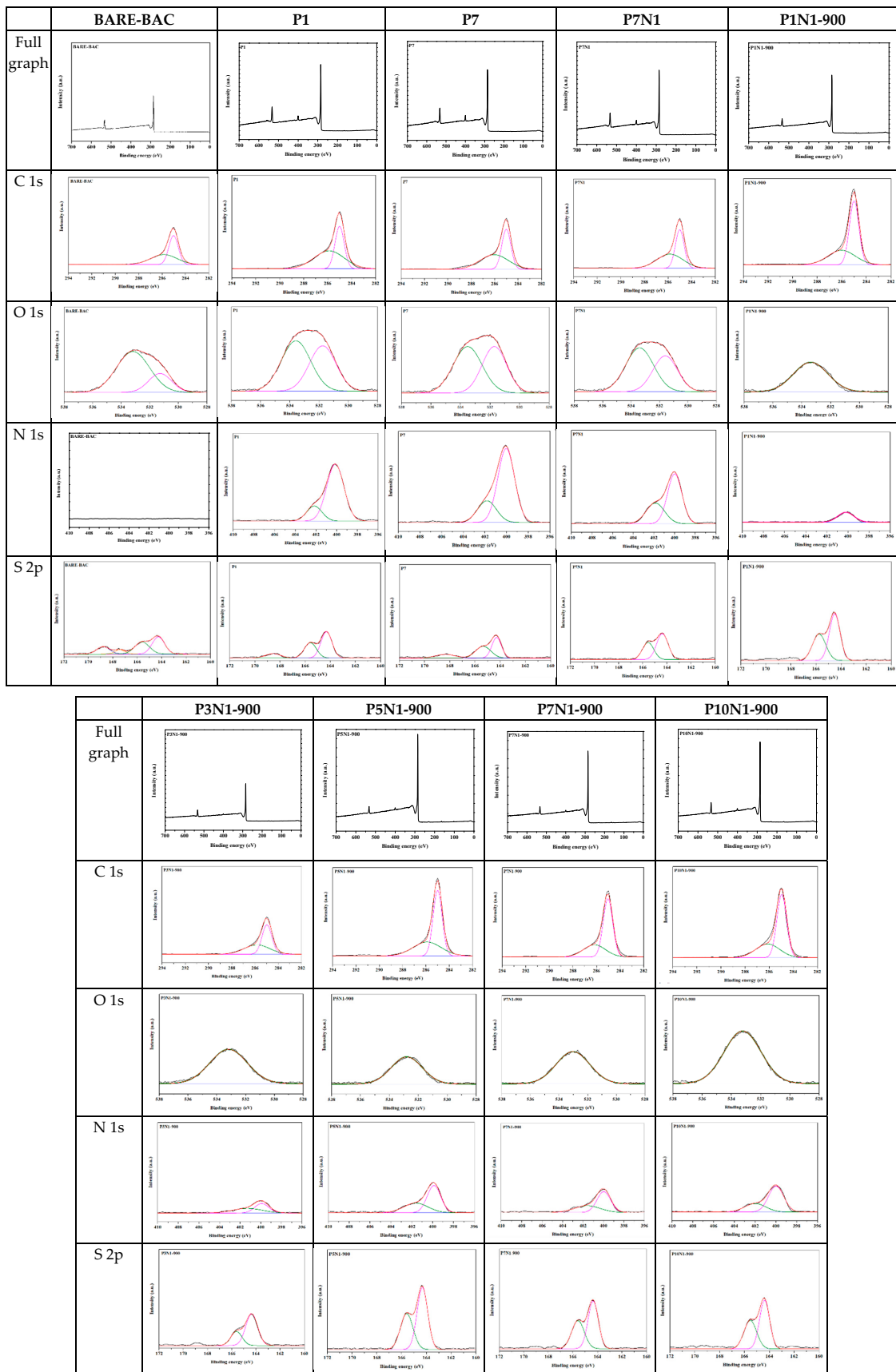


**Figure 4.** High resolution XPS spectra of C 1s, O 1s, N 1s, and S 2p for all BAC samples. (black line: experimental value, red line: fitting value).

After modification with piperazine, the number of N bonds increases, whereas the number of bonds involving S decreases. After heating and modification with piperazine and nitric acid, the number of N bonds increases, and the number of bonds involving O and S decreases.

The various N components in BAC were further determined by fitting the N 1s spectra. As shown in Figure 4 and Table 5, deconvolution of the N 1s spectrum reveals the presence of N-(C)<sub>3</sub> (tertiary nitrogen, secondary amine) and C-N<sup>+</sup>O-C (oxidized nitrogen functionalities). After piperazine treatment, the number of assigned N bonds increases, particularly the N-(C)<sub>3</sub> content, and thus, when only piperazine is used, it coats the BAC surface. By contrast, in the BAC treated with piperazine and nitric acid, the content of C-N<sup>+</sup>O-C increases by >50% and then decreases as the piperazine content increases. Thus, COOH groups are formed on the surface of the BAC via the addition of nitric acid, and piperazine is linked to these groups. The piperazine content of P1N1-900 is excessively low to link to the COOH groups, and thus, the content of N-(C)<sub>3</sub> is 100%. Conversely, in P3N1-900, piperazine and the COOH groups are linked, increasing the content of C-N<sup>+</sup>O-C. In P5N1-900, the COOH groups and piperazine are linked, the remaining piperazine is coated on the surface of the BAC, and the content of N-(C)<sub>3</sub> is increased. N atoms doped onto the BAC surface may react with CH<sub>3</sub>CHO to enhance its adsorption [30].

As shown in Figure 4 and Table 5, deconvolution of the O 1s and S 2p spectra reveal the presence of O-C/O-S (in phenol/epoxy or thioether/sulfonic acid), O=C/O=S (in carboxy/carbonyl or sulfoxides/sulfones), C-S-C (in sulfides), R-S-S-OR (in thioethers), R<sub>2</sub>-S=O (in sulfoxides), and R-SO<sub>2</sub>-R (in sulfones). During heating, the high temperature may convert O=C/O=S to O-C/O-S, and R<sub>2</sub>-S=O and R-SO<sub>2</sub>-R in P1N1-900–P10N1-900 are converted to C-S-C via heating. S doped on the BAC surface may also react with aldehydes to increase the HCHO adsorption performance [39].

**Table 6.** Results of the deconvolution of the XPS spectra of C 1s, O 1s, N 1s, and S 2p (in bold—atomic % of specific elements).

Bond Assignment	Energy [eV]	BARE-BAC [%]	P1 [%]	P7 [%]	P7N1 [%]	P1N1-900 [%]	P3N1-900 [%]	P5N1-900 [%]	P7N1-900 [%]	P10N1-900 [%]
<b>C 1s</b>										
C-C sp <sup>2</sup>	284.8	51.15	41.23	46.46	47.57	62.49	55.21	60.32	69.02	66.84
C-O (phenol, alcohol, ether), C=N (amine, amide)	286.0–286.3	48.85	58.77	53.54	52.43	37.51	44.79	39.68	30.98	33.16
<b>O 1s</b>										
O-C/O-S (in phenol/epoxy or thioethers/sulfonic)	533.3–533.6	77.78	55.29	54.16	59.19	100	100	100	100	100
O=C/O=S (in carboxy/carbonyl or sulfoxides/sulfones)	532.0–532.5	22.22	44.71	45.84	40.81	-	-	-	-	-
<b>N 1s</b>										
N-(C) <sub>3</sub> (tertiary nitrogen, secondary amine)	399.1–400.0	-	83.51	76.46	68.18	100	100	63.78	67.99	70.61
C-N <sup>+</sup> O-C (oxidized nitrogen functionalities)	402.3	-	16.49	23.54	31.82	-	-	36.22	32.01	29.39
<b>S 2p</b>										
C-S-C (in sulfides); R-S-S-OR (in thioethers)	164.5–166.0	81.74	96.35	93.56	93.56	100	100	100	100	100
R <sub>2</sub> -S=O (in sulfoxides)	167.0–167.3	2.28	-	-	-	-	-	-	-	-
R-SO <sub>2</sub> -R (in sulfones)	168.4–168.6	15.98	3.65	6.44	6.44	-	-	-	-	-

Sources: Adapted from [40].

### 3.2. CH<sub>3</sub>CHO Adsorption

Figure 5 shows the CH<sub>3</sub>CHO breakthrough curves measured at 10 °C in dry conditions, and the calculated adsorption parameters are listed in Table 6. The modified BAC samples display higher W<sub>ad</sub> values, as shown in Table 7, than that of the unmodified BAC: 17.17, 18.73, 50.05, 57.44, 18.84, 54.48, 62.95, 72.34, and 61.38 mg/g for BARE-BAC, P1, P7, P7N1, P1N1-900, P3N1-900, P5N1-900, P7N1-900, and P10N1-900, respectively. The samples co-impregnated with piperazine and nitric acid generally exhibit higher W<sub>ad</sub> values than those of the samples treated only with piperazine (P1 and P7). P7N1-900, in particular, adsorbs

the largest amount of  $\text{CH}_3\text{CHO}$ , which is 4.2-fold higher than that adsorbed by BARE-BAC. Physical factors, such as the high  $S_{\text{BET}}$  values of the modified BAC samples and abundant micropores, likely contribute to the adsorption performances of the co-impregnated BAC samples. Moreover, heating destroys the functional groups on the surface of the BAC and ensures that the active sites comprising piperazine and nitric acid are evenly distributed. As the piperazine content increases, the amount of adsorbed  $\text{CH}_3\text{CHO}$  increases, but when the piperazine content is excessive, as in P10N1-900, the pores of the BAC are blocked and the adsorption performance is reduced. Chemical factors, such as the addition of nitric acid, result in higher  $\text{CH}_3\text{CHO}$  adsorption. The chemical reactions between  $\text{CH}_3\text{CHO}$  and linked piperazine explain the increased  $\text{CH}_3\text{CHO}$  adsorption levels of the BAC samples co-impregnated with piperazine and nitric acid compared to those of the other samples. This is corroborated by the XPS spectra, which show that  $\text{CH}_3\text{CHO}$  reacts strongly with  $\text{C}-\text{N}^+\text{O}-\text{C}$  (oxidized nitrogen functionalities) and  $\text{N}-(\text{C})_3$  (tertiary nitrogen, secondary amine). The reaction with  $\text{CH}_3\text{CHO}$  is stronger when both types of bonds are present compared to that when one type is present. Figure 6 shows the comprehensive mechanisms of amine modification of the BAC and  $\text{CH}_3\text{CHO}$  adsorption on the modified BAC surface.

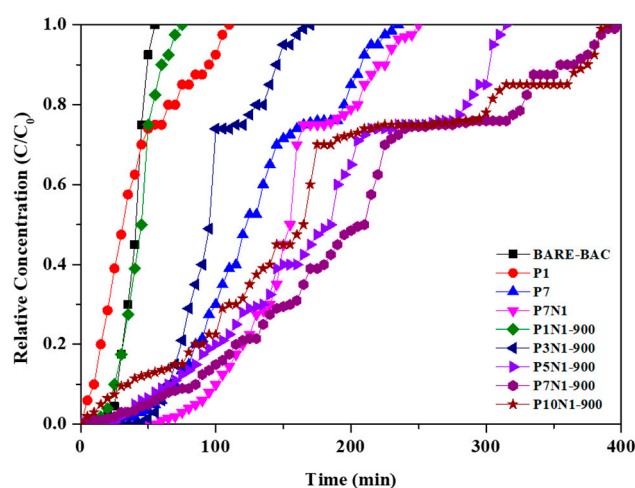


Figure 5.  $\text{CH}_3\text{CHO}$  breakthrough curves of all BAC samples.

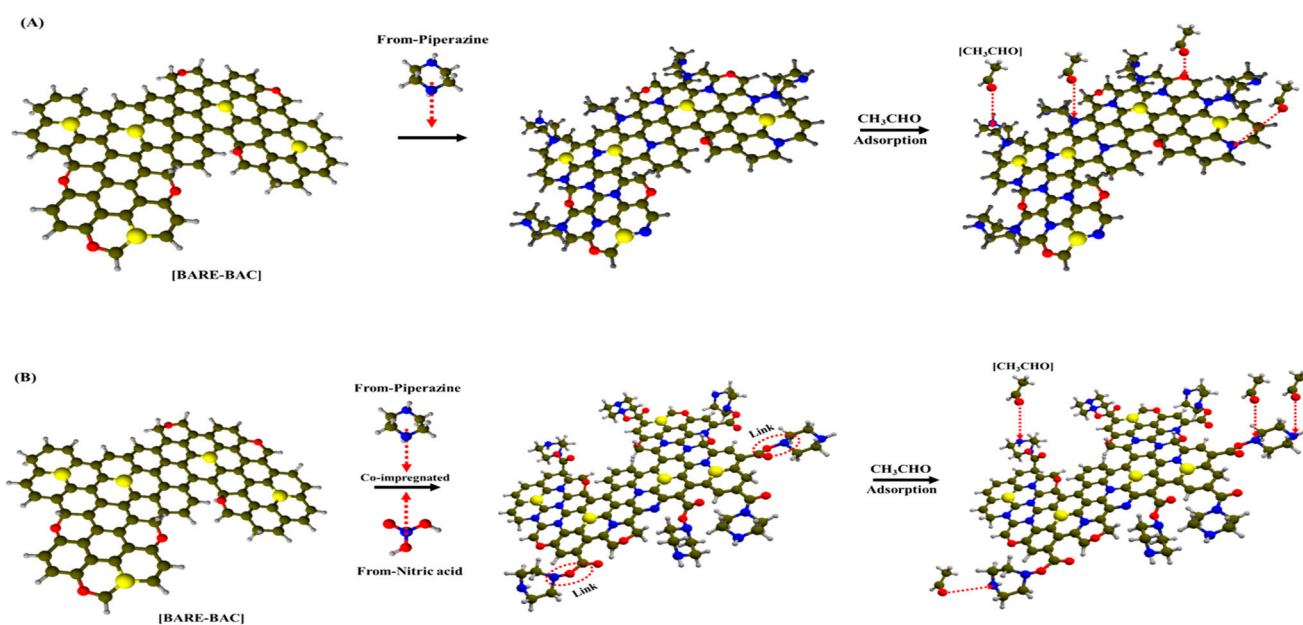


Figure 6. Conceptual diagram of (A) piperazine impregnated and (B) piperazine and nitric acid co-impregnated on the surface of BAC.

**Table 7.** CH<sub>3</sub>CHO adsorption parameters on all BAC samples.

Sample	C <sub>in</sub> [ppm]	W <sub>ad</sub> [mg/g]
BARE-BAC	200	17.17
P1	200	18.73
P7	200	50.05
P7N1	200	57.44
P1N1-900	200	18.84
P3N1-900	200	54.48
P5N1-900	200	62.95
P7N1-900	200	72.34
P10N1-900	200	61.38

**3.3. Effect of Thermal Regeneration on CH<sub>3</sub>CHO Adsorption**

Finally, we evaluated the thermal regeneration efficiencies of BARE-BAC and P7N1-900 after CH<sub>3</sub>CHO adsorption. The BAC samples were subjected to three cycles of CH<sub>3</sub>CHO adsorption and regeneration. Thermal regeneration was performed by heating the samples at 5 K/min to 453 K in a muffle furnace and maintaining this temperature for 2 h in air. Figure 7 shows the breakthrough curves obtained under dry conditions, and Table 8 presents the data. The results of Cycles 2 and 3 exhibit similar trends to those shown in Figure 5. As shown in Table 8, the respective regeneration efficiencies of BARE-BAC and P7N1-900 are 86.78% and 8.77%. Amine modification significantly reduces the regeneration efficiency of BARE-BAC by a factor of 10. BARE-BAC exhibits a high ratio of physical adsorption, whereas P7N1-900 displays a high ratio of chemical adsorption. BARE-BAC physisorbs CH<sub>3</sub>CHO and desorbs it well in all cycles. By contrast, P7N1-900 chemisorbs CH<sub>3</sub>CHO in Cycle 1 but does not desorb well, and thus, the CH<sub>3</sub>CHO adsorption declines significantly in Cycle 2. Meanwhile, the amounts of CH<sub>3</sub>CHO adsorbed in Cycles 2 and 3 are similar.

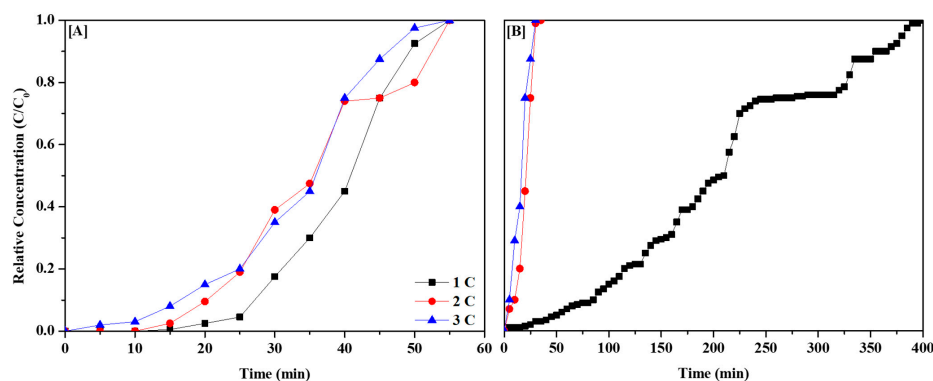


**Figure 7.** CH<sub>3</sub>CHO regeneration efficiency of 3 cycles: BARE-BAC (A) and P7N1-900 (B).

**Table 8.** CH<sub>3</sub>CHO regeneration efficiency of three cycles.

Sample	Number of Cycle	Adsorption Amount [mg/g]	Regeneration Efficiency of 3 Cycles [%]
BARE-BAC	1	17.17	86.78
	2	15.89	
	3	14.90	
P7N1-900	1	72.34	8.77
	2	6.13	
	3	5.97	

#### 4. Conclusions

Customized BAC was heated at 900 °C and impregnated with piperazine or binary piperazine/nitric acid to enhance CH<sub>3</sub>CHO removal via adsorption. The amount of piperazine was varied from 1 to 10% (*w/v*) and nitric acid was used at 1% (*w/v*). When only piperazine was used, the pore and micropore volumes of the modified BACs decreased with increasing piperazine content. The  $S_{\text{BET}}$  of BARE-BAC was 1442.1 m<sup>2</sup>/g, and that of P7 was reduced to 794.5 m<sup>2</sup>/g (modified BAC with 7% *w/v* impregnation of piperazine). Meanwhile, co-impregnation resulted in a minimized decrease in  $S_{\text{BET}}$ , e.g., 1347.2 m<sup>2</sup>/g for P1N1-900 (1% *w/v* each of piperazine and nitric acid, followed by heating at 900 °C). This suggests that nitric acid penetrates into the BAC microstructure to form pores of larger size and volume. However, the qualitative chemical structures of BARE-BAC and P7N1-900 (impregnation with 7% *w/v* piperazine and 1% *w/v* nitric acid, followed by heating at 900 °C) were not significantly different according to FTIR spectroscopy. Elemental analysis revealed that amine treatment increased the N contents of the BAC samples. When CH<sub>3</sub>CHO adsorption was performed at 10 °C under dry conditions, the adsorption performance of P7N1-900 increased 4.2-fold compared to that of BARE-BAC. This suggests that the chemical factors of BAC have a greater effect on CH<sub>3</sub>CHO adsorption than the physical factors. In regard to the impregnation with piperazine only (P1 and P7), the lower CH<sub>3</sub>CHO adsorption capacities could be explained by linkages to hidden amines and intrinsic COOH groups, resulting in negative effects on adsorption. By contrast, P1N1-900 and P7N1-900 should exhibit linked piperazine-amines but still contain carboxylic acids on the surfaces of the BAC samples, resulting in increased levels of CH<sub>3</sub>CHO adsorption. The CH<sub>3</sub>CHO adsorption capacity of BARE-BAC was 17.17 mg/g, and those of P7 and P7N1-900 increased to 50.05 and 72.34 mg/g, respectively. The XP spectra indicated that N-(C)<sub>3</sub> (tertiary nitrogen, secondary amine) and C-N<sup>+</sup>O-C (oxidized nitrogen functionalities) were present throughout the amine-treated BAC samples. The presence of C-N<sup>+</sup>O-C indirectly indicated that the amines were linked to COOH groups, which were mostly generated via nitric acid treatment. An increased amine content resulted in higher concentrations of N-(C)<sub>3</sub>, and thus, amine treatment introduced primary and secondary NH functional groups into the modified BAC and facilitated CH<sub>3</sub>CHO adsorption. Although CH<sub>3</sub>CHO adsorption was only evaluated under flow conditions, the modified BAC samples should display high CH<sub>3</sub>CHO adsorption capacities even under static conditions.

**Supplementary Materials:** The following supporting information can be downloaded at: <https://www.mdpi.com/article/10.3390/membranes13060595/s1>, Figure S1: SEM Morphology of Bare BAC, Figure S2: TEM Morphology of Bare BAC (After Grinding/Crushing BAC), Figure S3: XRD Patterns of Bare BAC, Figure S4: SEM-EDX of Bare BAC, Figure S5: Attrition and Abrasion Test of Bare BAC (Physical Stability), Figure S6: Acetaldehyde Cycle Test over Bare BAC, Figure S7: Particle Size Distribution of Bare BAC, Figure S8: CH<sub>2</sub>CHO Adsorption Parameters on Cucunut Shell and Coal Based Activated Carbon Samples.

**Author Contributions:** Conceptualization, Y.-J.K. (Yu-Jin Kang) and S.-J.Y.; methodology, Y.-J.K. (Yu-Jin Kang), D.-J.S., Y.-J.K. (Yu-Jin Kim) and H.-R.C.; validation, Y.-J.K. (Yu-Jin Kim) and K.O.; investigation, Y.-J.K. (Yu-Jin Kang), D.-J.S., Y.-J.K. (Yu-Jin Kim) and H.-R.C.; resources, S.-H.Y. and J.-I.P.; data curation, Y.-J.K. (Yu-Jin Kang) and K.O.; writing—original draft preparation, Y.-J.K. (Yu-Jin Kang); writing—review and editing, Y.-J.K. (Yu-Jin Kang) and Y.-J.K. (Yu-Jin Kim); visualization, Y.-J.K. (Yu-Jin Kang); supervision, S.-H.Y. and J.-I.P.; project administration, S.-H.Y. and J.-I.P. All authors have read and agreed to the published version of the manuscript.

**Funding:** This research was supported by the KNU-DP (Republic of Korea National University Development Project) funded by the Ministry of Education (MOE, Republic of Korea) and National Research Foundation of Republic of Korea (NRF).

**Institutional Review Board Statement:** Not applicable.

**Data Availability Statement:** The data presented in this study are available upon request from the corresponding author.

**Conflicts of Interest:** The authors declare no conflict of interest.

## References

1. Lee, H.W.; Kim, S.; Ryu, C.; Park, S.H.; Park, Y.K. Review of the use of activated biochar for energy and environmental applications. *Carbon Lett.* **2018**, *26*, 1–10.
2. Isinkaralar, K.; Turkyilmaz, A. Simultaneous adsorption of selected VOCs in the gas environment by low-cost adsorbent from *Ricinus communis*. *Carbon Lett.* **2022**, *32*, 1781–1789. [[CrossRef](#)]
3. Ryu, D.Y.; Kim, D.W.; Kang, Y.J.; Lee, Y.J.; Nakabayashi, K.; Miyawaki, J.; Park, J.I.; Yoon, S.H. Preparation of environmental-friendly N-rich chitin-derived activated carbon for the removal of formaldehyde. *Carbon Lett.* **2022**, *32*, 1473–1479. [[CrossRef](#)]
4. Lee, Y.J.; Lee, H.M.; Kim, B.J. Facile microwave treatment of activated carbons and its effects on hydrocarbon adsorption/desorption behaviors. *Carbon Lett.* **2023**, *33*, 1–10. [[CrossRef](#)]
5. Diana, P.; Alexander, O.; Tikhon, K.; Eugenii, G.; Elena, I.; Alexander, Z. Carbonization of oriented poly(vinyl alcohol) fibers impregnated with potassium bisulfate. *Carbon Lett.* **2020**, *30*, 637–650.
6. Azuma, K.; Uchiyama, I.; Uchiyama, S.; Kunugita, N. Assessment of inhalation exposure to indoor air pollutants: Screening for health risks of multiple pollutants in Japanese dwellings. *Environ. Res.* **2016**, *145*, 39–49. [[CrossRef](#)]
7. Ghaffarianhoseini, A.; AlWaer, H.; Omrany, H.; Ghaffarianhoseini, A.; Alalouch, C.; Clements-Croome, D.; Tookey, J. Sick building syndrome: Are we doing enough? *Archit. Sci. Rev.* **2018**, *61*, 99–121. [[CrossRef](#)]
8. Jansz, J. Theories and knowledge about sick building syndrome. *SBS* **2011**, *591*, 25–58.
9. Naddafi, K.; Nabizadeh, R.; Rostami, R.; Ghaffari, H.R.; Fazlzadeh, M. Formaldehyde and acetaldehyde in the indoor air of waterpipe cafés: Measuring exposures and assessing health effects. *Build. Environ.* **2019**, *165*, 106392. [[CrossRef](#)]
10. World Health Organization. Acetaldehyde: Health and safety guide. *Health Saf. Guide* **1994**, *90*, 32.
11. Nikawa, T.; Naya, S.I.; Tada, H. Rapid removal and decomposition of gaseous acetaldehyde by the thermo-and photo-catalysis of gold nanoparticle-loaded anatase titanium (IV) oxide. *J. Colloid Interface Sci.* **2015**, *456*, 161–165. [[CrossRef](#)]
12. Gabelman, A.; Hwang, S.T. Hollow fiber membrane contactors. *J. Membr. Sci.* **1999**, *159*, 61–106. [[CrossRef](#)]
13. Busca, G.; Berardinelli, S.; Resini, C.; Arrighi, L. Technologies for the removal of phenol from fluid streams: A short review of recent developments. *J. Hazard. Mater.* **2008**, *160*, 265–288. [[CrossRef](#)] [[PubMed](#)]
14. Kennes, C.; Thalasso, F. Waste gas biotreatment technology. *J. Chem. Technol. Biotechnol.* **1998**, *72*, 303–319. [[CrossRef](#)]
15. Lahousse, C.; Bernier, A.; Grange, P.; Delmon, B.; Papaefthimiou, P.; Ioannides, T.; Verykios, X. Evaluation of  $\gamma$ -MnO<sub>2</sub> as a VOC removal catalyst: Comparison with a noble metal catalyst. *J. Catal.* **1998**, *178*, 214–225. [[CrossRef](#)]
16. Parmar, G.R.; Rao, N.N. Emerging control technologies for volatile organic compounds. *Crit. Rev. Environ. Sci. Technol.* **2008**, *39*, 41–78. [[CrossRef](#)]
17. Gil, E.R.; Ruiz, B.; Lozano, M.S.; Martín, M.J.; Fuente, E. VOCs removal by adsorption onto activated carbons from biocollagenic wastes of vegetable tanning. *Chem. Eng. J.* **2014**, *245*, 80–88. [[CrossRef](#)]
18. Kang, Y.J.; Jo, H.K.; Jang, M.H.; Ma, X.; Jeon, Y.; Oh, K.; Park, J.I. A Brief Review of Formaldehyde Removal through Activated Carbon Adsorption. *Appl. Sci.* **2022**, *12*, 5025. [[CrossRef](#)]
19. Zaitan, H.; Manero, M.H.; Valdés, H. Application of high silica zeolite ZSM-5 in a hybrid treatment process based on sequential adsorption and ozonation for VOCs elimination. *J. Environ. Sci.* **2016**, *41*, 59–68. [[CrossRef](#)]
20. Kim, K.J.; Ahn, H.G. The effect of pore structure of zeolite on the adsorption of VOCs and their desorption properties by microwave heating. *Microporous Mesoporous Mater.* **2012**, *152*, 78–83. [[CrossRef](#)]
21. Liu, H.; Yu, Y.; Shao, Q.; Long, C. Porous polymeric resin for adsorbing low concentration of VOCs: Unveiling adsorption mechanism and effect of VOCs' molecular properties. *Sep. Purif. Technol.* **2019**, *228*, 115755. [[CrossRef](#)]
22. Bradley, R.H. Recent developments in the physical adsorption of toxic organic vapours by activated carbons. *Adsorpt. Sci. Technol.* **2011**, *29*, 1–28. [[CrossRef](#)]
23. Das, D.; Gaur, V.; Verma, N. Removal of volatile organic compound by activated carbon fiber. *Carbon* **2004**, *42*, 2949–2962. [[CrossRef](#)]
24. Singh, K.P.; Mohan, D.; Tandon, G.S.; Gupta, G.S.D. Vapor-phase adsorption of hexane and benzene on activated carbon fabric cloth: Equilibria and rate studies. *Ind. Eng. Chem.* **2002**, *41*, 2480–2486. [[CrossRef](#)]
25. Hayashi, T.; Kumita, M.; Otani, Y. Removal of acetaldehyde vapor with impregnated activated Carbons: Effects of steric structure on impregnant and acidity. *Environ. Sci. Technol.* **2005**, *39*, 5436–5441. [[CrossRef](#)]
26. Vikrant, K.; Qu, Y.; Kim, K.H.; Boukhvalov, D.W.; Ahn, W.S. Amine-functionalized microporous covalent organic polymers for adsorptive removal of a gaseous aliphatic aldehyde mixture. *Environ. Sci. Nano* **2020**, *7*, 3447–3468. [[CrossRef](#)]
27. Yamashita, K.; Noguchi, M.; Mizukoshi, A.; Yanagisawa, Y. Acetaldehyde removal from indoor air through chemical absorption using L-cysteine. *Int. J. Environ. Res. Public Health* **2010**, *7*, 3489–3498. [[CrossRef](#)] [[PubMed](#)]
28. Son, B.C.; Park, C.H.; Kim, C.S. Fabrication of antimicrobial nanofiber air filter using activated carbon and cinnamon essential oil. *J. Nanosci. Nanotechnol.* **2020**, *20*, 4376–4380. [[CrossRef](#)] [[PubMed](#)]
29. El-Sayed, Y.; Bandosz, T.J. A study of acetaldehyde adsorption on activated carbons. *J. Colloid Interface Sci.* **2001**, *242*, 44–51. [[CrossRef](#)]
30. El-Sayed, Y.; Bandosz, T.J. Acetaldehyde adsorption on nitrogen-containing activated carbons. *Langmuir* **2002**, *18*, 3213–3218. [[CrossRef](#)]

31. Park, K.H.; Shim, W.G.; Shon, H.K.; Lee, S.G.; Ngo, H.H.; Vigneswaran, S.; Moon, H. Adsorption characteristics of acetaldehyde on activated carbons prepared from corn-based biomass precursor. *Sep. Sci. Technol.* **2010**, *45*, 1084–1091. [[CrossRef](#)]
32. Branton, P.; Bradley, R.H. Effects of active carbon pore size distributions on adsorption of toxic organic compounds. *Adsorption* **2011**, *17*, 293–301. [[CrossRef](#)]
33. Baur, G.B.; Yuranov, I.; Kiwi-Minsker, L. Activated carbon fibers modified by metal oxide as effective structured adsorbents for acetaldehyde. *Catal. Today* **2015**, *249*, 252–258. [[CrossRef](#)]
34. Ryu, D.Y.; Nakabayashi, K.; Shimohara, T.; Morio, U.; Mochida, I.; Miyawaki, J.; Jeon, Y.; Park, J.I.; Yoon, S.H. Behaviors of cellulose-based activated carbon fiber for acetaldehyde adsorption at low concentration. *Appl. Sci.* **2019**, *10*, 25. [[CrossRef](#)]
35. Kim, B.J.; An, K.H.; Shim, W.G.; Park, Y.K.; Park, J.; Lee, H.; Jung, S.C. Acetaldehyde Adsorption Characteristics of Ag/ACF Composite Prepared by Liquid Phase Plasma Method. *Nano Mater.* **2021**, *11*, 2344. [[CrossRef](#)] [[PubMed](#)]
36. Park, S.; Yaqub, M.; Lee, S.; Lee, W. Adsorption of acetaldehyde from air by activated carbon and carbon fibers. *Environ. Eng. Res.* **2022**, *27*, 2. [[CrossRef](#)]
37. Ramezanipour Penchah, H.; Ghaemi, A.; Jafari, F. Piperazine-modified activated carbon as a novel adsorbent for CO<sub>2</sub> capture: Modeling and characterization. *Environ. Sci. Pollut. Res.* **2022**, *29*, 5134–5143. [[CrossRef](#)]
38. Karnati, S.R.; Høgsaa, B.; Zhang, L.; Fini, E.H. Developing carbon nanoparticles with tunable morphology and surface chemistry for use in construction. *Constr. Build. Mater.* **2020**, *262*, 120780. [[CrossRef](#)]
39. Kang, Y.J.; Jo, H.K.; Jang, M.J.; Han, G.J.; Yoon, S.J.; Oh, K.; Park, J.I. Acid treatment enhances performance of beads activated carbon for formaldehyde removal. *Carbon Lett.* **2023**, *33*, 397–408. [[CrossRef](#)]
40. Seredych, M.; Łoś, S.; Giannakoudakis, D.A.; Rodríguez-Castellón, E.; Bandosz, T.J. Photoactivity of g-C<sub>3</sub>N<sub>4</sub> /S-Doped Porous Carbon Composite: Synergistic Effect of Composite Formation. *ChemSusChem* **2016**, *9*, 795–799. [[CrossRef](#)]

**Disclaimer/Publisher’s Note:** The statements, opinions and data contained in all publications are solely those of the individual author(s) and contributor(s) and not of MDPI and/or the editor(s). MDPI and/or the editor(s) disclaim responsibility for any injury to people or property resulting from any ideas, methods, instructions or products referred to in the content.